Chapter 7

Electromagnetic Metamaterial Absorbers: From Narrowband to Broadband

Weiren Zhu

Additional information is available at the end of the chapter

http://dx.doi.org/10.5772/intechopen.78581

Abstract

Metamaterial perfect absorbers have received significant attention owing to their ability of achieving complete absorption of the electromagnetic waves with deeply subwavelength profiles. In this chapter, we will present a general review of the recent progress on theories, designs, and characterizations of metamaterial absorbers. We will first review the fundamental theories and design guidelines for achieving perfect absorption in subwavelength metamaterials. Several typical narrowband metamaterial absorbers are then presented with nearly 100% absorptivities. Next, we will focus on the realizations of broadband and frequency-tunable metamaterial absorbers. Coherent perfect absorbers, whose absorption performances are controllable via the interference of two counter-propagating electromagnetic waves, will also been introduced. In particular, we will also focus on the recent achievements of metamaterial absorbers in our research group.

Keywords: metamaterial absorbers, perfect absorption, coherent perfect absorbers, tunable, multiband, ultra-broadband

1. Introduction

Metamaterials, also known as artificially structured materials, have attracted extensive attention in the last decade, owing to their exotic properties that are not readily available in nature [1–4]. The basic idea of a metamaterial is to design subwavelength unit cells, also known as meta-atoms or meta-molecules, having novel electric and/or magnetic responses to the incident electromagnetic waves [5–7]. This enables the availability of artificial mediums with arbitrary effective material parameters. The development of metamaterials results in a series of intriguing applications, such as a cloak of invisibility [8, 9], giant optical chirality [10, 11], wave-front control [12, 13], surface plasmon manipulations [14–16], as well as antennas of

compact sizes and enhanced directionalities [17–19]. It is well known that one of the main obstacles toward practical engineering applications is the inevitable intrinsic loss in metamaterials. A significant amount of effort has been devoted to achieving low-loss devices through optimizing structural geometries [20–22]. Loss compensation using gain elements [23–25] is another scheme which requires external excitation sources.

On the other hand, absorption is also highly desired in many applications, such as energy harvesting [26], scattering reduction [27], as well as thermal sensing [28]. By utilizing the full usefulness of loss, metamaterials with nearly uniform absorption are achievable through properly engineering the electric and magnetic resonances [29–35]. Due to the resonance nature, the first reported metamaterial-based perfect absorber is of narrow bandwidth and polarization sensitive, which restrict its usefulness in practical applications [29]. Great efforts have been devoted to expanding the bandwidth of metamaterial absorbers. Metamaterials with multiband absorption have later been developed using multiple resonant unit cells and combining them through a co-plane arrangement [36, 37]. When these resonances are closed to each other in frequency, broadband absorption is achievable [38]. Broadband absorption can also be achieved in metamaterial absorbers with multi-layer structures [39, 40] or using vertically standing nanowires [41, 42]. Moreover, by incorporating active mediums, the absorptivities and frequencies of metamaterial absorbers could be adjusted via external biases [43, 44].

In this chapter, we present a brief review on the fundamental theories and recent evolutions in the research field of electromagnetic metamaterial absorbers, whose operating frequencies cover from microwave, THz, infrared, to visible regimes. The rest of this chapter is organized as follows. Section 2 introduces the general theories on the design of metamaterial absorbers, where impedance matching theory and multiple interference theory are introduced. Section 3 reviews the narrowband metamaterial absorbers of various structures, all of which have nearly uniform absorptivities. Next, the technologies for broadening the bandwidths of metamaterial absorbers are presented in Section 4. Metamaterial absorbers with tunable absorption properties are reviewed in Section 5. Moreover, the coherent control of the metamaterial absorber's absorptivity through phase modulation is discussed in Section 6. Finally, the conclusion is given.

2. Theoretical scheme of metamaterial absorbers

We start by reviewing general theories that explain the origin and underlying physics for achieving perfect absorption in metamaterials. The first theory is by designing both electric and magnetic resonances in a metamaterial, so that the effective permittivity and permeability of the metamaterial can be tailored for achieving impedance matching with free space [45, 46]. In such a case, no reflection occurs at the interface and the entire incident energy has a chance to be absorbed inside the metamaterial absorber. The other theory is based on the destructive interference of multiple-order reflections due to the multiple inner reflections inside the dielectric substrate.

2.1. Impedance matching theory

A metamaterial absorber is typically a sandwiched structure, consisting of an array of certain metallic patterns on one side of a substrate and backed with a highly conductive metallic

ground plane. The electric permittivity and magnetic permeability of the metamaterial are $\varepsilon = \varepsilon_0 \varepsilon_r(\omega)$ and $\mu = \mu_0 \mu_r(\omega)$, respectively. Here, ε_0 and μ_0 are the free space permittivity and permeability. $\varepsilon_r(\omega)$ and $\mu_r(\omega)$ are the frequency-dependent relative permittivity and permeability of the medium, which are unitless and normalized with respect to the values of free space. Due to the presence of the ground plane, no transmittance could be found on the other side of the metamaterial. This allows us to focus only on the reflection from the metamaterial.

According to the Fresnel formula of reflection, the reflectivity (R) from the metamaterial is [29]

$$R_{\mathrm{TE}} = |r_{\mathrm{TE}}|^2 = \left| \frac{\mu_r \cos\theta - \sqrt{n^2 - \sin\theta}}{\mu_r \cos\theta + \sqrt{n^2 - \sin\theta}} \right|^2, \tag{1}$$

$$R_{\mathrm{TM}} = |r_{\mathrm{TM}}|^2 = \left| \frac{\varepsilon_r \cos\theta - \sqrt{n^2 - \sin\theta}}{\varepsilon_r \cos\theta + \sqrt{n^2 - \sin\theta}} \right|^2, \tag{2}$$

where the subscripts TE and TM refer to transverse electric (TE) and transverse magnetic (TM) polarized waves, θ is the angle of incidence, and $n = \sqrt{\varepsilon_r \mu_r}$ is the effective refractive index of the metamaterial. For the case of normal incident, we have $\theta = 0^\circ$, so that these equations reduce to:

$$R = \left| \frac{Z - Z_0}{Z + Z_0} \right|^2 = \left| \frac{\sqrt{\mu_r} - \sqrt{\varepsilon_r}}{\sqrt{\mu_r} + \sqrt{\varepsilon_r}} \right|^2, \tag{3}$$

with $Z = \sqrt{\mu/\varepsilon}$ being the impedance of the metamaterial and $Z_0 = \sqrt{\mu_0/\varepsilon_0}$ being the impedance of free space. Since the metallic ground leads to zero transmissivity, the absorptivity arrives:

$$A = 1 - R = 1 - \left| \frac{Z - Z_0}{Z + Z_0} \right|^2 = 1 - \left| \frac{\sqrt{\mu_r} - \sqrt{\varepsilon_r}}{\sqrt{\mu_r} + \sqrt{\varepsilon_r}} \right|^2. \tag{4}$$

The above equation indicates that impedance matching, $Z = Z_0$ or $\mu_r = \varepsilon_r$, is a critical condition for achieving perfect absorption. It is worth noting that, to achieve impedance matching in a metamaterial absorber, simultaneous electric and magnetic resonances are required. For a metamaterial with single resonance, either electric or magnetic resonance, its impedance will be strong mismatched with that of free space. As a consequence, no perfect absorber would be found.

2.2. Interference theory

A metamaterial absorber can be regarded as a coupled system and, particularly, its magnetic resonance is induced due to the anti-parallel currents between the front and back metallic layers. However, we may also independently consider the functionalities of the front meta-layer and the ground plane on the other side [47]. The front layer with certain metallic patterns functions as a partial reflection surface, which can be utilized to modify the complex reflection and

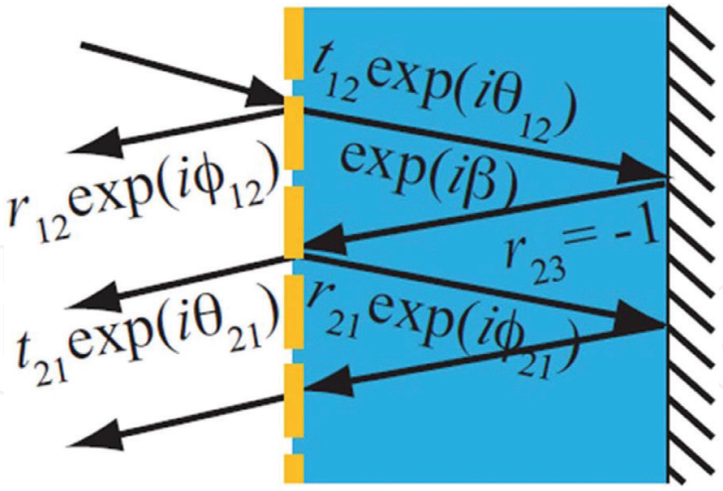

Figure 1. Multiple reflections and interference model of metamaterial absorber. The yellow dashed line refers the resonator array. Reproduced from [47] with permission.

transmission coefficients. On the other hand, the highly conductive ground plane works as a perfect reflector, offering a phase delay of 180° to the electromagnetic wave reflecting on it.

As shown in **Figure 1**, the front meta-layer resides at the interface between air and the dielectric substrate. The incident electromagnetic wave is partially reflected back to air with a reflection coefficient $\tilde{r}_{12}(\omega) = r_{12}(\omega)\, e^{i\varphi_{12}(\omega)}$ and partially transmitted into the substrate with a transmission coefficient $\tilde{t}_{12}(\omega) = t_{12}(\omega)\, e^{i\theta_{12}(\omega)}$. The transmitted wave will propagate further until reaching the metallic ground plane. The complex propagation constant inside the dielectric substrate is $\tilde{\beta} = \beta_1 + i\beta_2 = \sqrt{\varepsilon_d}\, k_0 d$, where k_0 is the wavenumber of free space, d is the thickness of the substrate, β_1 represents the propagation phase, and β_2 refers to the absorption in the dielectric substrate. At the ground plane, a total reflection occurs with a reflection coefficient of −1. After direct mirror reflection and an additional propagation phase delay $\tilde{\beta}$, partial reflection and transmission occur again at the front interface. The corresponding reflection and transmission coefficients are $\tilde{r}_{21}(\omega) = r_{21}(\omega)\, e^{i\varphi_{21}(\omega)}$ and $\tilde{t}_{21}(\omega) = t_{21}(\omega)\, e^{i\theta_{21}(\omega)}$, respectively. It is worth noting that multiple reflections and transmissions exist inside the dielectric substrate, and the totally output energy at the left side of the metamaterial is the superposition of reflections of all orders:

$$\tilde{r}(\omega) = \tilde{r}_{12}(\omega) \frac{\tilde{t}_{12}(\omega)\, \tilde{t}_{21}(\omega)\, e^{2i\tilde{\beta}}}{1 + \tilde{r}_{21}(\omega)\, e^{2i\tilde{\beta}}}, \tag{5}$$

where the first term in the right is the reflection directly from the meta-layer, and the second term is the contribution of the superposition of the multiple higher-order reflections. As long as we know the total reflection $\tilde{r}$, the absorption spectrum of the metamaterial absorber could be obtained by $A(\omega) = 1 - |\tilde{r}(\omega)|^2$. The interference theory can well explain the features observed in those metamaterial absorbers with metallic grounds and also provide an alternative understanding of the origin and underlying physics of metamaterial absorbers.

It is worth noting that the above analysis is fully based on the assumption that the incident wave is normal to the metamaterial. For the case when an electromagnetic wave incident is

http://dx.doi.org/10.5772/intechopen.78581

oblique with an angle θ, the propagation length inside the dielectric substrate becomes longer. Therefore, the propagation phase delay should be modified as $\tilde{\beta} = \sqrt{\varepsilon_d} k_0 d'$, where $d' = d/\cos\theta'$ is the modified propagation length inside the substrate and the refractive angle θ' can be obtained following Snell's law $\sqrt{\varepsilon_d}\sin\theta' = \sin\theta$ [48].

3. Narrowband metamaterial absorbers

The first metamaterial absorber was theoretically investigated in 2006, consisting of an array of split ring resonators (SRRs)-backed with a resistive sheet [49]. The incident wave is parallel to the SRR plane with magnetic field being perpendicular to the SRR array. Such an SRR array is placed on a resistive sheet having a resistance of 377 Ω for impedance matching with free space, similar to a Salisbury screen. Both the reflection and transmission are below −20 dB at the vicinity of 2 GHz as numerically found. This is due to the strong resonances in this structure, where nearly perfect absorption was achieved at this frequency. However, due to the standing arrangement of the SRR array, this structure is not of low profile as compared with planar structures, which also increase its complexity in the manufacture. The bandwidth of absorption is also very limited. Nevertheless, the design of this metamaterial absorption motivates further research in these kinds of absorbers.

In 2008, Landy et al. [29] proposed a planar sandwiched structure that consists of electric ring resonators and cut wires separated by an FR-4 substrate, as shown in **Figure 2**. This is the first-reported metamaterial absorber with a planar and deeply subwavelength structure. The absorptivity observed is as high as 96% at 11.65 GHz in simulation and 88% at 11.5 GHz in experiment. The relative bandwidth of full width half maximum (FWHM) is around 4%. The front electric ring resonators couple strongly to the incident electric field and contribute electric response, while the circulating flow of antiparallel surface currents at the front and back metallic layers contributed a magnetic response. The absorption intensity and frequency could be controlled by adjusting the geometric parameters of electric ring resonators or the

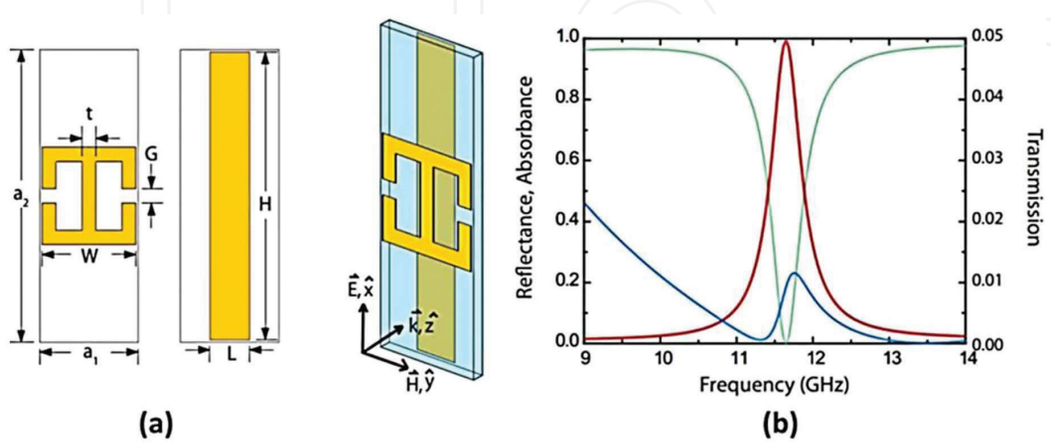

Figure 2. (a) Unit cell of the first planar metamaterial absorber, (b) simulated reflection, transmission, and absorptance at microwave frequency. Reproduced from [29] with permission.

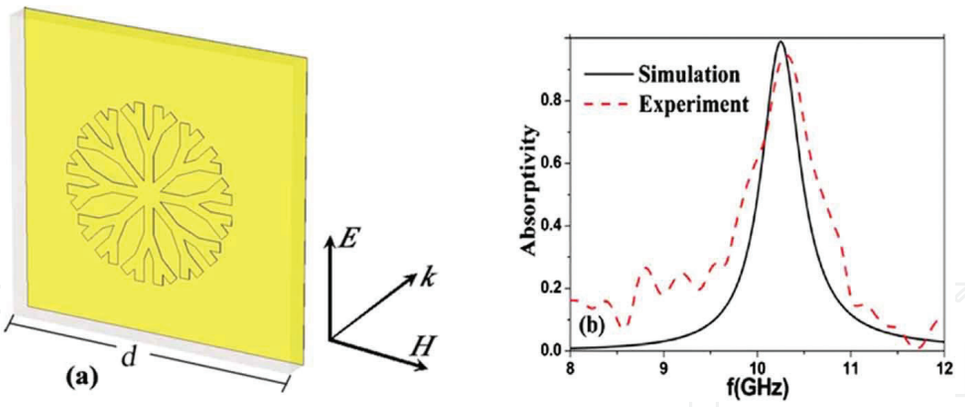

Figure 3. (a) Unit cell of dendritic metamaterial absorber and (b) simulated and measured absorptivity spectra. Reproduced from [50] with permission.

thickness of the substrate. Inspired by this pioneer work, great amounts of efforts have been devoted to the realization of metamaterial absorbers in different spectral ranges [30–40].

The initial metamaterial absorbers are polarization sensitive because of anisotropic unit cells [29, 51]. Planar metamaterial absorbers with highly symmetric structures were developed later, such as annular and circular patch arrays [52] and snowflake cells [53, 54]. In 2009, we developed a metamaterial absorber composed of dendritic unit cells [50]. As shown in **Figure 3(a)**, the periodical array of metallic dendritic cells is on one side of the FR-4 substrate and a full ground plane on the other side. It is shown in **Figure 3(b)** that both the simulation and experiment, in accordance with each other, show over 95% absorptivity at the frequency of 10.26 GHz. Such a metamaterial absorber has an excellence of planar isotropy, which shows equal absorption performance for an incident wave with arbitrary polarizations. When scaling down the size of the dendritic metamaterial absorber to the nanoscale, it is able to achieve perfect absorption in the optical regime, which was also confirmed with numerical simulation [50].

Metamaterials, including those metamaterial absorbers, are commonly made of periodically arranged unit cells. The imperfection in manufacture will, to some extent, affects the performance of the metamaterial. This is particularly significant in an optical regime where the unit cells of the metamaterials are of nano-scale. To study this effect, the impact of disorder in the unit-cell arrangement in the metamaterial absorber was further studied [55]. It was found that absorptivity decreases and the absorption frequency gets red-shift as the unit cells become more disorderly. However, the metamaterial absorber with random unit cells still presents over 95% absorptivity for a reasonable level of disorder.

4. Broadband metamaterial absorbers

Various techniques have been developed for expanding the bandwidth of metamaterial absorbers. The major techniques for bandwidth enhancement includes the use of multi-layer stacked structures [39, 40], a co-planar arrangement of multiple resonant cells [56, 57], as well as adding lumped elements [58]. Highly lossy dielectrics or semiconductors have also been

http://dx.doi.org/10.5772/intechopen.78581

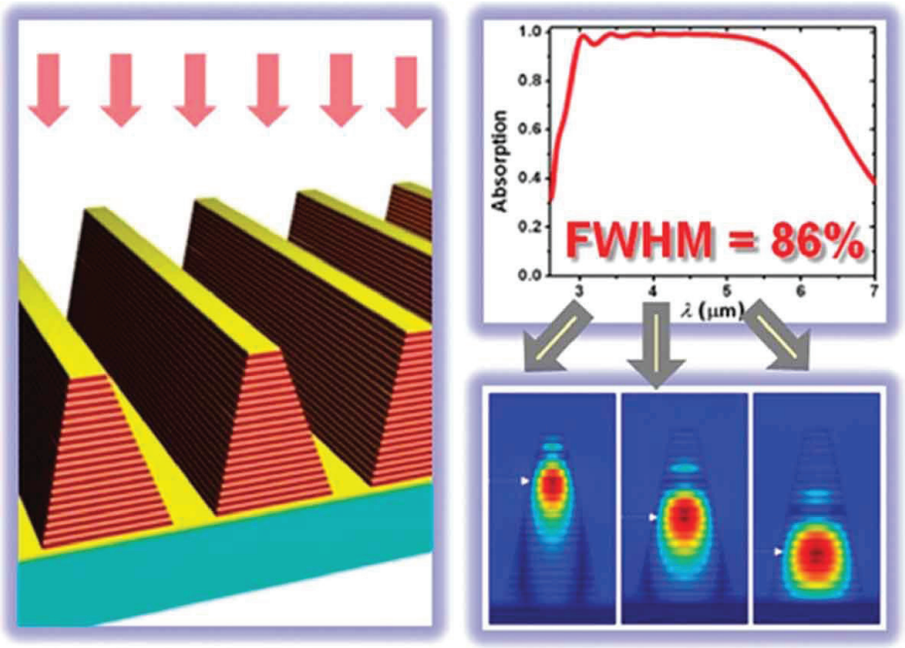

Figure 4. Schematic view of the saw-toothed metamaterial absorber and its absorption spectrum. Reproduced from [39] with permission.

widely used for designing broadband metamaterial absorbers [59, 60]. In this section, some typical approaches for designing bandwidth-enhanced absorbers are discussed.

One of the most effective approaches for designing broadband metamaterial absorber is to stack resonant patches of different sizes. Cui et al. [39] proposed a multi-layer saw-toothed anisotropic metamaterial absorber at infrared wavelengths, as shown in **Figure 4**. Although such a metamaterial absorber is made of 21 layers of metal patches, its total thickness is still reasonably thin compared to the operating wavelength. Particularly, they demonstrated that the relative full absorptivity width at half maximum could be achieved to a figure as high as 86%. The ultra-broad bandwidth in such a layered metamaterial absorber is realized by the overlapping of multiple resonances according to the metal patches at different layers. Electromagnetic waves of higher frequencies are absorbed at the upper parts, while those of lower frequencies are trapped at the lower parts.

Intrinsic high loss in dielectrics or semiconductors can also be utilized for designing wide-band absorption in simple structures [59, 60]. For example, water is a highly lossy dielectric at microwave frequencies, whose permittivity could be well described by the Debye formula [62]. **Figure 5** shows the metamaterial absorber made of a water layer (with periodical holes) placed in a resin container, which is backed with a metallic ground plane at the bottom. With such a structure, Xie et al. [61] experimentally demonstrated an ultra-broadband absorption with absorptivity higher than 90% in the entire frequency band from 12 to 29.6 GHz. To figure out whether the broadband absorption in such a water metamaterial absorber is predominantly because of the intrinsic high loss of water, they also compared the absorption spectra for the case when the full water layer without holes and the case when the resin container is empty of water. As shown in **Figure 5(d)**, they found that the absorptivity of a full water layer

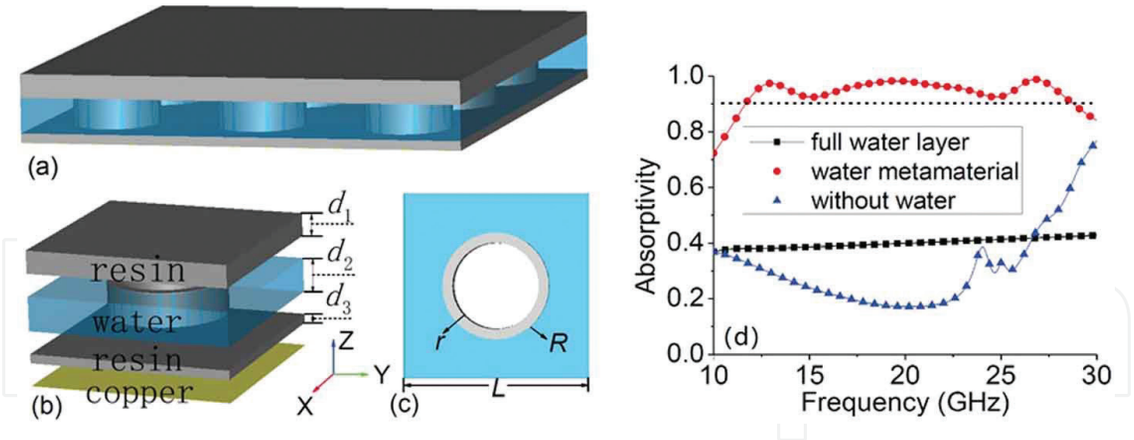

Figure 5. (a) Schematic view of the water metamaterial absorber, (b) layer by layer view of the unit cell, and (c) cut plane view of the water layer. (d) Absorptivity spectra of the water metamaterial absorber, the full water layer backed by a metal ground, and the metamaterial without water. Reproduced from [61] with permission.

is only around 35–40%, while the absorptivity of the metamaterial absorber reduces to be only around 20–40% when the water is emptied. These results confirm that the ultra-broadband absorption mainly contributes to localized resonances in the structured water resonators.

Highly doped silicon has relatively low resistivity and behaves as a lossy dielectric at terahertz frequencies, which was employed for achieving broadband absorption [59]. Using a lossy patterned silicon substrate, Yin et al. [64] also experimentally demonstrated a metamaterial absorber with an operating band from 0.9 to 2.5 THz. A silicon-based metamaterial absorber, as shown in **Figure 6(a)**, was proposed for broadband high absorption at visible wavelengths [63]. Such a metamaterial absorber has three functional layers: a subwavelength silicon layer with periodic truncated conical holes, a subwavelength silicon dioxide spacer, and a thick gold substrate. As seen from the numerical results in **Figure 6(c)**, the silicon metamaterial absorber with truncated conical holes has higher absorptivity and wider bandwidth at the frequency band of interest.

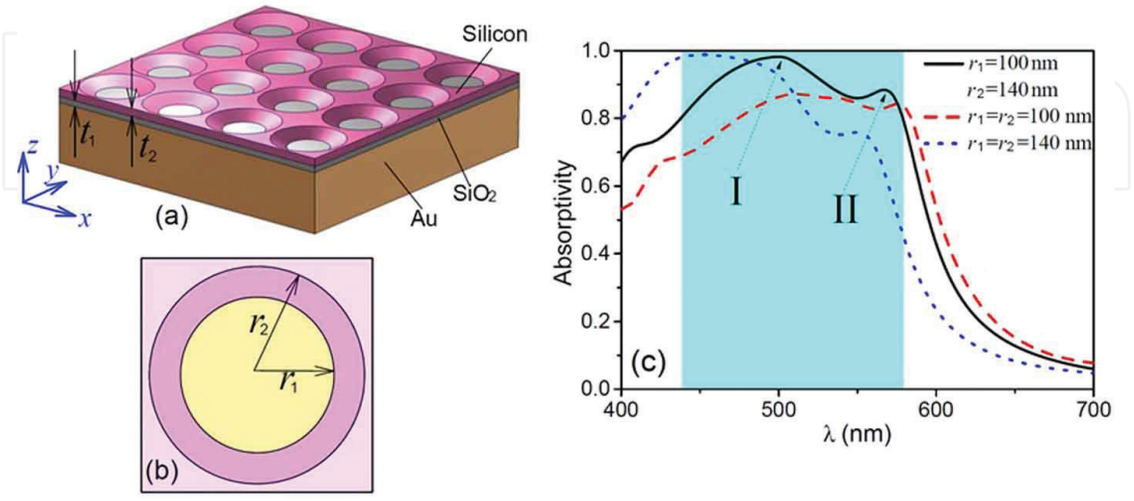

Figure 6. (a) Schematic view of the silicon-based metamaterial absorber and (b) its unit cell. (c) Absorptivity spectra of silicon-based metamaterials with conical and circular holes. Reproduced from [63] with permission.

5. Frequency tunable metamaterial absorbers

Although metamaterials, in principle, can be designed for having arbitrary electromagnetic properties, these properties are generally fixed after the design of the metamaterials [65–68]. This is also true for metamaterial-based absorbers, whose operating frequencies are very much fixed, restricting their practical applications. Therefore, metamaterial absorbers with frequency-tunable characteristics are highly desirable, which allows more fruitful applications. To enable the tunability in a metamaterial absorber, one may integrate a medium with adjustable material properties into a traditional passive metamaterial absorber. Some of the proven methods include having elements, such as varactor diodes [69], ferroelectrics [70], ferrites [71], graphene [72, 73], anisotropic liquid crystals [74], and phase-transition materials [75].

Mechanical bending or shifting was also studied for tunable metamaterial absorbers [74–78]. Zhang et al. [76] experimentally presented a mechanically stretchable metamaterial absorber, which is composed of dielectric resonators on a thin conductive rubber layer, as shown in **Figure 7**. A nearly 100% absorption was found, along with strong localized electric field confinement due to the Mie-type resonance of the dielectric resonators. When stretching the metamaterial absorber under uniaxial stress, the space between dielectric bricks increases gradually, and therefore the resonance frequency undergoes a red-shift of 410 MHz in the X band (see **Figure 7**). Zhu et al. [78] experimentally demonstrated a metamaterial absorber whose resonance frequency can be shifted by mechanical means. The shift was achieved by

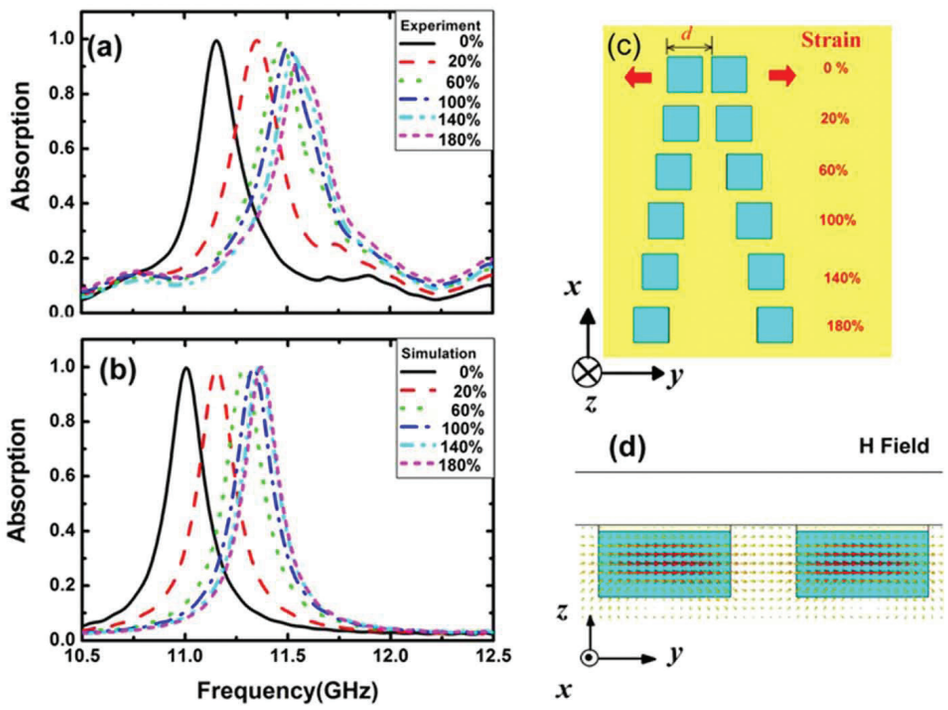

Figure 7. (a) Experimental and (b) simulated absorptivity spectra of the mechanically stretchable dielectric metamaterial absorber. (c) Schematic of stretching the dielectric resonators on a thin conductive rubber layer. (d) Magnetic field distribution at the resonance frequency. Reproduced from [76] with permission.

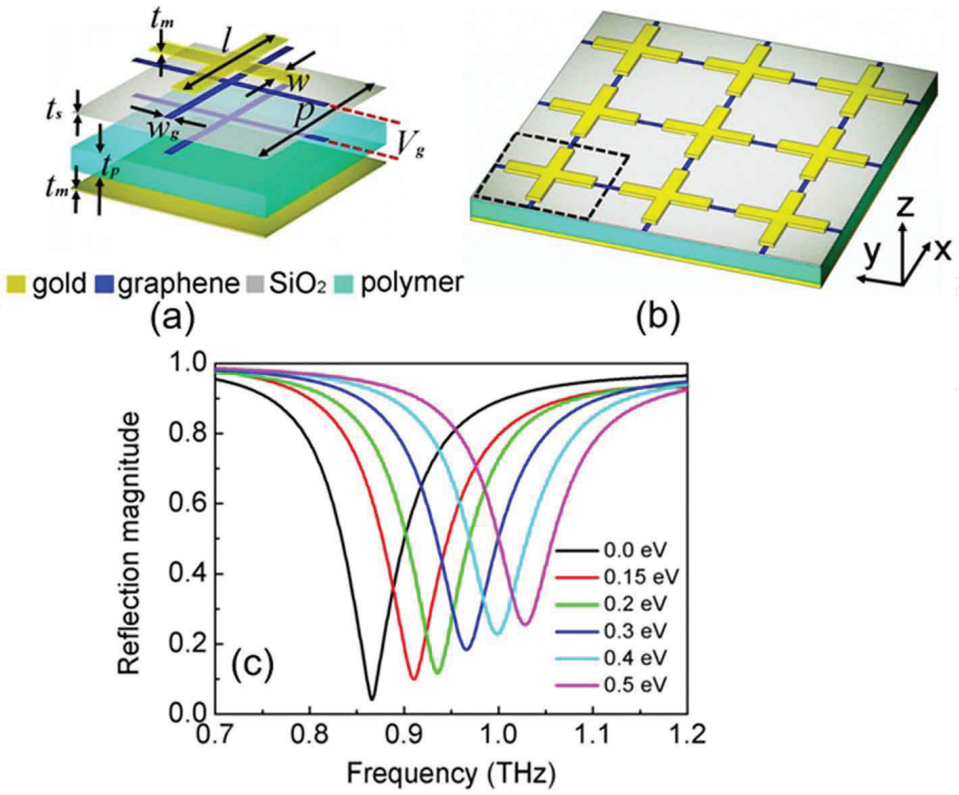

Figure 8. (a) Cross-shaped unit cell with graphene wires and (b) schematic view of the metamaterial absorber. (c) Absorptivity of the metamaterial absorber under different bias voltages. Reproduced from [79] with permission.

adding an auxiliary dielectric slab parallel to the metamaterial absorber and varying the gap between the metamaterial and the slab. They also demonstrated the possibility of creating multiple absorption bands by smartly adjusting the size and shape of the dielectric slab.

Graphene has also been utilized for designing tunable metamaterial absorbers due to its tunability of surface conductivity [80, 81]. Zhang et al. [79] combined the metamaterial absorber having cross-shaped metallic unit cells with graphene wires, as shown in **Figures 8(a)** and **8(b)**. Such a structure was realized for polarization insensitive absorption and the absorption spectral could be tuned at terahertz frequencies. As shown in **Figure 8(c)**, they demonstrated that the absorption peak frequency is able to be tuned within a 15% frequency range with nearly uniform peak absorptivity, by simply controlling the Fermi level of graphene. The Fermi level in graphene can be conveniently controlled by adjusting the bias voltage on the graphene layers.

6. Coherent metamaterial absorbers

It is known that one of drawbacks of a typical metamaterial absorber is that the absorptivity is commonly fixed after the initial design of the metamaterial absorber. As a consequence, it is not suitable for environments that require the flexible tunability of absorption. The presence of coherent perfect absorption (CPA) is a solution for this issue [82, 83]. Mathematically, CPA corresponds to a zero eigenvalue of the scattering matrix S at a specific frequency, which can

be regarded as the time-reversed lasing at threshold. The perfect absorption can be achieved by utilizing the destructive interference in a standing wave system formed by two counter-propagating beams [84]. Moreover, the absorptivity in such a system can be modulated from nearly 0 to 100% by solely adjusting the phase difference between the two counter-propagating incident beams [85]. Owing to this dynamic configurability of absorptivity, such absorbers are very attractive for applications in transducers, modulators, and electromagnetic switches.

The concept of CPA was first presented theoretically by Chong et al. [82] and experimentally demonstrated by the same group later [83]. Since then, CPA phenomena have been observed in epsilon-near-zero metamaterials [86], slow light waveguides [87], a metasurface consisting of metallic cross antennas [88], and a Fano resonance plasmonic system [84], just to name a few.

Most of the coherent metamaterial absorbers are based on metallic subwavelength resonators. However, recent researches revealed that CPA could also be achieved in metal-free metamaterials or metasurfaces. Zhu et al. [89] designed a mono-layer fishnet structure made of all dielectric ceramic, which has a thickness of two levels smaller than the operating wavelength. They demonstrated that CPA could be found in such a structure and the absorptivity is controllable within a wide range from 0.38 to 99.85% through phase modulation. A similar monolayer fishnet structure made of water could also be used for achieving high coherent absorption at multiple frequency bands [90]. Moreover, due to intrinsic high loss in water, the CPA could be designed with wider bandwidths.

Unlike perfect metamaterial absorbers that require strong electric and magnetic resonances resulting from the artificially structured resonators, few recent works reported that CPA can also be found in naturally existing layer materials with deep subwavelength thickness. Li et al. [89] presented that ultra-thin conductive films could be used for achieving CPA. As demonstrated experimentally, broadband coherent absorption with relative bandwidth close to 100% at microwave frequencies was observed in a conductive film, having a thickness of 1/1000 of the working wavelength. The CPA phenomena in thin graphene and MoS_2 layers were also investigated [60, 91]. The tunable conductivity in graphene or MoS_2 allows such a coherent absorber to be more flexible in working frequency, which could be controlled by adjusting the chemical doping rate or bias voltage.

7. Conclusions

Since the first design in 2008, metamaterial perfect absorbers with deeply subwavelength profiles have received significant attention in the last decade. In this chapter, we have presented a comprehensive review of the recent progress on the theories and designs of planar metamaterial absorbers. We reviewed the fundamental theories and design guidelines for achieving perfect absorption in subwavelength metamaterials. Different structures of unit cells have been studied for achieving nearly complete absorptions. The realizations of broadband and frequency-tunable metamaterial absorbers were also discussed. Moreover, we introduced the concept of coherent perfect absorbers and the coherent control of absorptivity via phase modulation in such metamaterial absorbers. A significant number of works reviewed in this chapter were done in our research group.

Acknowledgements

This work was supported by National Natural Science Foundation of China (61701303), Natural Science Foundation of Shanghai (17ZR1414300), and Shanghai Pujiang Program (17PJ1404100).

Author details

Weiren Zhu

Address all correspondence to: weiren.zhu@sjtu.edu.cn

Department of Electronic Engineering, Shanghai Jiao Tong University, Shanghai, China

References

[1] Engheta N, Ziolkowski RW. Metamaterials: Physics and Engineering Explorations. New Jersey: John Wiley & Sons; 2006

[2] Shelby RA, Smith DR, Schultz S. Experimental verification of a negative index of refraction. Science. 2001;**292**:77-79

[3] Valentine J, Zhang S, Zentgraf T, Ulin-Avila E, Genov DA, Bartal G, Zhang X. Three-dimensional optical metamaterial with a negative refractive index. Nature. 2008;**455**: 376-379

[4] Baimuratov AS, Pereziabova TP, Zhu W, Leonov MY, Baranov AV, Fedorov AV, Rukhlenko ID. Optical anisotropy of topologically distorted semiconductor nanocrystals. Nano Letters. 2017;**17**:5514-5520

[5] Zhang X, Liu Z. Superlenses to overcome the diffraction limit. Nature Materials. 2008;**7**:435-441

[6] Kang M, Zhu W, Rukhlenko ID. Experimental observation of the topological structure of exceptional points in an ultrathin hybridized metamaterial. Physical Review A. 2017;**96**:063823

[7] Zhu W, Rukhlenko ID, Xiao F, Premaratne M. Polarization conversion in U-shaped chiral metamaterial with four-fold symmetry breaking. Journal of Applied Physics. 2014;**115**:143101

[8] Schurig D, Mock JJ, Justice BJ, Cummer SA, Pendry JB, Starr AF, Smith DR. Metamaterial electromagnetic cloak at microwave frequencies. Science. 2006;**314**:977-980

[9] Zhu W, Shadrivov I, Powell D, Kivshar Y. Hiding in the corner. Optics Express. 2011;**19**:20827-20832

[10] Wang B, Zhou J, Koschny T, Kafesaki M, Soukoulis CM. Chiral metamaterials: Simulations and experiments. Journal of Optics A. 2009;**11**:114003

[11] Zhu W, Rukhlenko ID, Huang Y, Wen G, Premaratne M. Wideband giant optical activity and negligible circular dichroism of near-infrared chiral metamaterial based on a complementary twisted configuration. Journal of Optics. 2013;**15**:125101

[12] Kang M, Wang HT, Zhu W. Wavefront manipulation with a dipolar metasurface under coherent control. Journal of Applied Physics. 2017;**122**:013105

[13] Cui TJ, Qi MQ, Wan X, Zhao J, Chen Q. Coding metamaterials, digital metamaterials and programmable metamaterials. Light: Science and Applications. 2014;**3**:e218

[14] Liu Y, Zentgraf T, Bartal G, Zhang X. Transformational plasmon optics. Nano Letters. 2010;**10**:1991-1997

[15] Zhu W, Rukhlenko ID, Premaratne M. Linear transformation optics for plasmonics. Journal of the Optical Society of America B: Optical Physics. 2012;**29**:2659-2664

[16] Zhu W, Rukhlenko ID, Premaratne M. Maneuvering propagation of surface plasmon polaritons using complementary medium inserts. IEEE Photonics Journal. 2012;**4**:741-748

[17] Hong W, Jiang ZH, Yu C, Zhou J, Chen P, Yu Z, Zhang H, Yang B, Pang X, Jiang M, Cheng Y, Al-Nuaimi MKT, Zhang Y, Chen J, He S. Multibeam antenna technologies for 5G wireless communications. IEEE Transactions on Antennas and Propagation. 2017;**65**:6231-6249

[18] Si L-M, Zhu W, Sun H-J. A compact, planar, and CPW-fed metamaterial-inspired dual-band antenna. IEEE Antennas and Wireless Propagation Letters. 2013;**12**:305-308

[19] Lin FH, Chen ZN. Low-profile wideband metasurface antennas using characteristic mode analysis. IEEE Transactions on Antennas and Propagation. 2017;**65**:1706-1713

[20] Cao W, Singh R, Al-Naib IA, He M, Taylor AJ, Zhang W. Low-loss ultra-high-Q dark mode plasmonic fano metamaterials. Optics Letters. 2012;**37**:3366-3368

[21] Zhu W, Zhao X. Numerical study of low-loss cross left-handed metamaterials at visible frequency. Chinese Physics Letters. 2009;**26**:074212

[22] Zhu W, Zhao X. Adjusting the resonant frequency and loss of dendritic left-handed metamaterials with fractal dimension. Journal of Applied Physics. 2009;**106**:093511

[23] Xiao S, Drachev VP, Kildishev AV, Ni X, Chettiar UK, Yuan H-K, Shalaev VM. Loss-free and active optical negative-index metamaterials. Nature. 2010;**446**:735-738

[24] Premaratne M, Agrawal GP. Light Propagation in Gain Media: Optical Amplifiers. Cambridge: Cambridge University Press; 2011

[25] Zhu W, Rukhlenko ID, Premaratne M. Light amplification in zero-index metamaterial with gain inserts. Applied Physics Letters. 2012;**101**:031907

[26] Wang H, Sivan PV, Mitchell A, Rosengarten G, Phelan P, Wang L. Highly efficient selective metamaterial absorber for high-temperature solar thermal energy harvesting. Solar Energy Materials & Solar Cells. 2015;**137**:235-242

[27] Culhaoglu AE, Osipov AV, Russer P. Mono- and bistatic scattering reduction by a metamaterial low reflection coating. IEEE Transactions on Antennas and Propagation. 2013;**61**:462-466

[28] Guddala S, Kumar R, Ramakrishna SA. Thermally induced nonlinear optical absorption in metamaterial perfect absorbers. Applied Physics Letters. 2015;**106**:111901

[29] Landy NI, Sajuyigbe S, Mock JJ, Smith DR, Padilla WJ. Perfect metamaterial absorber. Physical Review Letters. 2008;**100**:207402

[30] Watts CM, Liu X, Padilla WJ. Metamaterial electromagnetic wave absorbers. Advanced Materials. 2012;**24**:OP98-OP120

[31] Zhu W, Zhao X, Gong B, Liu L, Su B. Optical metamaterial absorber based on leaf-shaped cells. Applied Physics A: Materials Science & Processing. 2011;**102**:147-151

[32] Huang Y, Wen G, Li J, Zhong J, Wang P, Sun Y, Gordona O, Zhu W. Metamaterial absorbers realized in X-band rectangular waveguide. Chinese Physics B. 2012;**21**:117801

[33] Zhu W, Rukhlenko ID, Premaratne M. Graphene metamaterial for optical reflection modulation. Applied Physics Letters. 2013;**102**:241914

[34] Ra'di Y, Simovski CR, Tretyakov SA. Thin perfect absorbers for electromagnetic waves: Theory, design, and realizations. Physical Review Applied. 2015;**3**:037001

[35] Liu X, Starr T, Starr AF, Padilla WJ. Infrared spatial and frequency selective metamaterial with near-unity absorbance. Physical Review Letters. 2014;**104**:207403

[36] Park JW, Tuong PV, Rhee JY, Kim KW, Jang WH, Choi EH, Chen LY, Lee YP. Multiband metamaterial absorber based on the arrangement of donut-type resonators. Optics Express. 2014;**104**:207403

[37] Zhou W, Wang P, Wang N, Jiang W, Dong X, Hu S. Microwave metamaterial absorber based on multiple square ring structures. AIP Advances. 2015;**5**:117109

[38] Gu S, Su B, Zhao X. Planar isotropic broadband metamaterial absorber. Journal of Applied Physics. 2013;**104**:163702

[39] Cui Y, Fung KH, Xu J, Ma H, Jin Y, He S, Fang NX. Ultrabroadband light absorption by a sawtooth anisotropic metamaterial slab. Nano Letters. 2012;**12**:1443-1447

[40] Kim YJ, Yoo YJ, Kim KW, Rhee JY, Kim YH, Lee YP. Dual broadband metamaterial absorber. Optics Express. 2015;**23**:3861-3868

[41] Shen Y, Pang Y, Wang J, Ma H, Pei Z. Ultra-broadband terahertz absorption by uniaxial anisotropic nanowire. IEEE Photonics Technology Letters. 2015;**27**:2284-2287

[42] Chen Q, Gu J, Liu P, Xie J, Wang J, Liu Y, Zhu W. Nanowire-based ultra-wideband absorber for visible and ultraviolet light. Optics and Laser Technology. 2018;**105**:102-105

[43] Chen H-T, O'Hara JF, Azad AK, Taylor AJ, Averitt RD, Shrekenhamer DB, Padilla WJ. Experimental demonstration of frequency-agile terahertz metamaterials. Nature Photonics. 2008;**2**:295-298

[44] Yao G, Ling F, Yue J, Luo C, Ji J, Yao J. Dual-band tunable perfect metamaterial absorber in the THz range. Optics Express. 2016;**24**:1518-1527

[45] Tao H, Landy NI, Bingham CM, Zhang X, Averitt RD, Padilla WJ. A metamaterial absorber for the terahertz regime: Design, fabrication and characterization. Optics Express. 2008;(10):7181-7188

[46] Li J, Wang F, Wen G, Huang Y, Zhu W. Planar metamaterial for matched waveguide termination. ACES Journal. 2013;**28**:1236-1243

[47] Chen H-T. Interference theory of metamaterial perfect absorbers. Optics Express. 2012;**20**:7165-7172

[48] Wanghuang T, Chen W, Huang Y, Wen G. Analysis of metamaterial absorber in normal and oblique incidence by using interference theory. AIP Advances. 2013;**3**:102118

[49] Bilotti F, Nucci L, Vegni L. An SRR based microwave absorber. Microwave and Optical Technology Letters. 2006;**48**:2171-2175

[50] Zhu W, Zhao X. Metamaterial absorber with dendritic cells at infrared frequencies. Journal of the Optical Society of America B: Optical Physics. 2009;**26**:2382-2385

[51] Diem M, Koschny T, Soukoulis CM. Wide-angle perfect absorber/thermal emitter in the terahertz regime. Physical Review B. 2009;**79**:033101

[52] Zhu W, Zhao X, Bao S, Zhang Y. Highly symmetric planar metamaterial absorbers based on annular and circular patches. Chinese Physics Letters. 2010;**27**:014204

[53] Huang Y, Wen G, Li J, Zhu W, Wang P, Sun Y. Wide-angle and polarization-independent metamaterial absorber based on snowflake-shaped configuration. Journal of Electromagnetic Waves and Applications. 2013;**27**:552-559

[54] Huang Y, Tian Y, Wen G, Zhu W. Experimental study of absorption band controllable planar metamaterial absorber using asymmetrical snowflake-shaped configuration. Journal of Optics. 2013;**15**:055104

[55] Zhu W, Zhao X. Metamaterial absorber with random dendritic cells. European Physical Journal Applied Physics. 2010;**50**:21101

[56] Bouchon P, Koechlin C, Pardo F, Haïdar R, Pelouard J-L. Wideband omnidirectional infrared absorber with a patchwork of plasmonic nanoantennas. Optics Letters. 2012;**37**: 1038-1040

[57] Liu Y, Gu S, Luo C, Zhao X. Ultra-thin broadband metamaterial absorber. Applied Physics A: Materials Science & Processing. 2012;**108**:19-24

[58] Cheng YZ, Wang Y, Nie Y, Gong RZ, Xiong X, Wang X. Design, fabrication and measurement of a broadband polarization-insensitive metamaterial absorber based on lumped elements. Journal of Applied Physics. 2012;**111**:044902

[59] Pu M, Wang M, Hu C, Huang C, Zhao Z, Wang Y, Luo X. Engineering heavily doped silicon for broadband absorber in the terahertz regime. Optics Express. 2012;**20**:25513-25519

[60] Zhu W, Xiao F, Kang M, Sikdar D, Liang X, Geng J, Premaratne M, Jin R. MoS_2 broadband coherent perfect absorber for terahertz waves. IEEE Photonics Journal. 2016;**8**:5502207

[61] Xie J, Zhu W, Rukhlenko ID, Xiao F, He C, Geng J, Liang X, Jin R, Premaratne M. Water metamaterial for ultra-broadband and wide-angle absorption. Optics Express. 2018;**26**: 5052-5059

[62] Ellison W. Permittivity of pure water, at standard atmospheric pressure, over the frequency range 0-25 THz and the temperature range 0-100°C. Journal of Physical and Chemical Reference Data. 2007;**36**:1-18

[63] Zhu W, Xiao F, Rukhlenko ID, Geng J, Liang X, Premaratne M, Jin R. Wideband visible-light absorption in an ultrathin silicon nanostructure. Optics Express. 2017;**25**:5781-5786

[64] Yin S, Zhu J, Xu W, Jiang W, Yuan J, Yin G, Xie L, Ying Y, Ma Y. High-performance terahertz wave absorbers made of silicon-based metamaterials. Applied Physics Letters. 2015;**107**:073903

[65] Smith DR, Padilla WJ, Vier DC, Nemat-Nasser SC, Schultz S. Composite medium with simultaneously negative permeability and permittivity. Physical Review Letters. 2000;**84**:4184-4187

[66] Plum E, Fedotov VA, Zheludev NI. Optical activity in extrinsically chiral metamaterial. Applied Physics Letters. 2008;**93**:191911

[67] Zhong J, Huang Y, Wen G, Sun H, Gordon O, Zhu W. Dual-band negative permittivity metamaterial based on cross circular loop resonator with shorting stubs. IEEE Antennas and Wireless Propagation Letters. 2012;**11**:803-806

[68] Fan J, Sun G, Zhu W. Electric and magnetic dipole couplings in split ring resonator metamaterials. Chinese Physics B. 2011;**20**:114101

[69] Wen Q-Y, Zhang H-W, Yang Q-H, Chen Z, Long Y, Jing Y-L, Lin Y, Zhang P-X. A tunable hybrid metamaterial absorber based on vanadium oxide films. Journal of Physics D: Applied Physics. 2012;**45**:235106

[70] Hand TH, Cummer SA. Frequency tunable electromagnetic metamaterial using ferroelectric loaded split rings. Journal of Applied Physics. 2008;**103**:066105

[71] Huang Y, Wen G, Zhu W, Li J, Si L, Premaratne M. Electrically tunable metasurface perfect absorbers for ultrathin mid-infrared optical modulators. Optics Express. 2014;**22**: 16408-16417

[72] Linder J, Halterman K. Graphene-based extremely wide-angle tunable metamaterial absorber. Scientific Reports. 2016;**6**:31225

[73] Yao Y, Shankar R, Kats MA, Song Y, Kong J, Loncar M, Capasso F. Electrically tunable metasurface perfect absorbers for ultrathin mid-infrared optical modulators. Nano Letters. 2014;**14**:6526-6532

[74] Shrekenhamer D, Chen W-C, Padilla WJ. Liquid crystal tunable metamaterial absorber. Physical Review Letters. 2013;**110**:177403

[75] Mkhitaryan VK, Ghosh DS, Rude M, Canet-Ferrer J, Maniyara RA, Gopalan KK, Pruneri V. Tunable complete optical absorption in multilayer structures including $Ge_2Sb_2Te_5$ without lithographic patterns. Advanced Optical Materials. 2017;**5**:1600452

[76] Zhang F, Feng S, Qiu K, Liu Z, Fan Y, Zhang W, Zhao Q, Zhou J. Mechanically stretchable and tunable metamaterial absorber. Applied Physics Letters. 2015;**106**:091907

[77] Pitchappa P, Ho CP, Kropelnicki P, Singh N, Kwong D-L, Lee C. Micro-electromechanically switchable near infrared complementary metamaterial absorber. Applied Physics Letters. 2014;**104**:201114

[78] Zhu W, Huang Y, Rukhlenko ID, Wen G, Premaratne M. Configurable metamaterial absorber with pseudo wideband spectrum. Optics Express. 2012;**20**:6616-6621

[79] Zhang Y, Feng Y, Zhu B, Zhao J, Jiang T. Graphene based tunable metamaterial absorber and polarization modulation in terahertz frequency. Optics Express. 2014;**24**:22743-22734

[80] Zhu W, Xiao F, Kang M, Sikdar D, Premaratne M. Tunable terahertz left-handed metamaterial based on multi-layer graphene-dielectric composite. Applied Physics Letters. 2014;**104**:051902

[81] Zhu W, Rukhlenko ID, Si L, Premaratne M. Graphene-enabled tunability of optical fishnet metamaterial. Applied Physics Letters. 2013;**102**:121911

[82] Chong YD, Ge L, Cao H, Stone AD. Coherent perfect absorbers: Time-reversed lasers. Physical Review Letters. 2010;**105**:053901

[83] Wan W, Chong YD, Ge L, Noh H, Stone AD, Cao H. Time-reversed lasing and interferometric control of absorption. Science. 2011;**331**:889-892

[84] Kang M, Chong YD, Wang H-T, Zhu W, Premaratne M. Critical route for coherent perfect absorption in a fano resonance plasmonic system. Applied Physics Letters. 2014;**105**:131103

[85] Pu M, Feng Q, Wang M, Hu C, Huang C, Ma X, Zhao Z, Wang C, Luo X. Ultrathin broadband nearly perfect absorber with symmetrical coherent illumination. Optics Express. 2012;**20**:2246-2254

[86] Feng S, Halterman K. Coherent perfect absorption in epsilon-near-zero metamaterials. Physical Review B. 2012;**86**:165103

[87] Gutman N, Sukhorukov AA, Chong YD, de Sterke CM. Coherent perfect absorption and reflection in slow-light waveguides. Optics Letters. 2013;**38**:4970-4973

[88] Kang M, Liu F, Li T-F, Guo Q-H, Li J, Chen J. Polarization-independent coherent perfect absorption by a dipole-like metasurface. Optics Letters. 2013;**38**:3086-3088

[89] Zhu W, Xiao F, Kang M, Premaratne M. Coherent perfect absorption in an all-dielectric metasurface. Applied Physics Letters. 2016;**108**:121901

[90] Zhu W, Rukhenko ID, Xiao F, He C, Geng J, Liang X, Premaratne M, Jin R. Multiband coherent perfect absorption in a water-based metasurface. Optics Express. 2017;**25**:15737-15745

[91] Fan Y, Zhang F, Zhao Q, Wei Z, Li H. Tunable terahertz coherent perfect absorption in a monolayer graphene. Optics Letters. 2014;**39**:6269-6272

IntechOpen